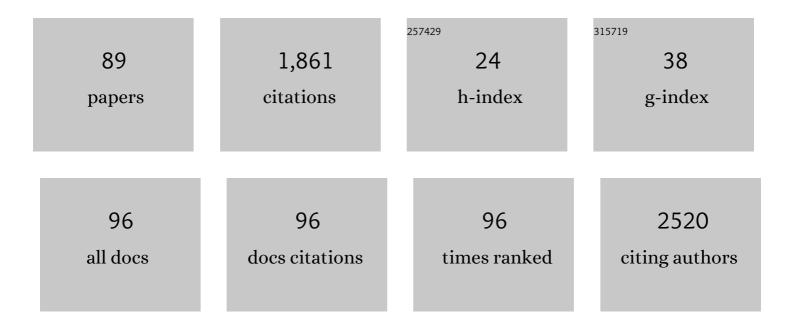
List of Publications by Year in descending order

Source: https://exaly.com/author-pdf/6189387/publications.pdf Version: 2024-02-01



#	Article	IF	CITATIONS
1	Pharmacokinetic and pharmacodynamic assessment of histamine H3 receptor occupancy by enerisant: a human PET study with a novel H3 binding ligand, [11C]TASP457. European Journal of Nuclear Medicine and Molecular Imaging, 2022, 49, 1127-1135.	6.4	3
2	Patterns of Distribution of 18F-THK5351 Positron Emission Tomography in Alzheimer's Disease Continuum. Journal of Alzheimer's Disease, 2022, 85, 223-234.	2.6	4
3	Brain 5-HT2A receptor binding and its neural network related to behavioral inhibition system. Brain Imaging and Behavior, 2022, 16, 1337-1348.	2.1	4
4	First-in-human in vivo imaging and quantification of monoacylglycerol lipase in the brain: a PET study with 18F-T-401. European Journal of Nuclear Medicine and Molecular Imaging, 2022, 49, 3150-3161.	6.4	3
5	[11C]NCGG401, a novel PET ligand for imaging of colony stimulating factor 1 receptors. Bioorganic and Medicinal Chemistry Letters, 2022, 65, 128704.	2.2	9
6	PET-based classification of corticobasal syndrome. Parkinsonism and Related Disorders, 2022, 98, 92-98.	2.2	5
7	Excess tau PET ligand retention in elderly patients with major depressive disorder. Molecular Psychiatry, 2021, 26, 5856-5863.	7.9	15
8	Differential associations of dopamine synthesis capacity with the dopamine transporter and D2 receptor availability as assessed by PET in the living human brain. NeuroImage, 2021, 226, 117543.	4.2	9
9	High-Contrast InÂVivo Imaging of Tau Pathologies in Alzheimer's and Non-Alzheimer's Disease Tauopathies. Neuron, 2021, 109, 42-58.e8.	8.1	157
10	Biodistribution and radiation dosimetry of the positron emission tomography probe for AMPA receptor, [11C]K-2, in healthy human subjects. Scientific Reports, 2021, 11, 1598.	3.3	8
11	PET imaging of colony-stimulating factor 1 receptor: A head-to-head comparison of a novel radioligand, ¹¹ C-GW2580, and ¹¹ C-CPPC, in mouse models of acute and chronic neuroinflammation and a rhesus monkey. Journal of Cerebral Blood Flow and Metabolism, 2021, 41, 2410-2422.	4.3	36
12	Relationship between regional gray matter volumes and dopamine D 2 receptor and transporter in living human brains. Human Brain Mapping, 2021, 42, 4048-4058.	3.6	3
13	Dynamic alterations in the central glutamatergic status following food and glucose intake: <i>in vivo</i> multimodal assessments in humans and animal models. Journal of Cerebral Blood Flow and Metabolism, 2021, 41, 2928-2943.	4.3	4
14	Evaluation of PiB visual interpretation with CSF AÎ ² and longitudinal SUVR in J-ADNI study. Annals of Nuclear Medicine, 2020, 34, 108-118.	2.2	7
15	Brain pharmacokinetics and biodistribution of 11C-labeled isoproterenol in rodents. Nuclear Medicine and Biology, 2020, 86-87, 52-58.	0.6	5
16	PET/CT for Neuroinflammation. , 2020, , 217-228.		1
17	SPECT and PET of the Brain. , 2020, , 211-231.		0
18	Synthesis of (R,S)-isoproterenol, an inhibitor of tau aggregation, as an 11C-labeled PET tracer via reductive alkylation of (R,S)-norepinephrine with [2-11C]acetone. Bioorganic and Medicinal Chemistry Letters, 2019, 29, 2107-2111.	2.2	3

#	Article	IF	CITATIONS
19	Correction of head movement by frame-to-frame image realignment for receptor imaging in positron emission tomography studies with [11C]raclopride and [11C]FLB 457. Annals of Nuclear Medicine, 2019, 33, 916-929.	2.2	5
20	PET-detectable tau pathology correlates with long-term neuropsychiatric outcomes in patients with traumatic brain injury. Brain, 2019, 142, 3265-3279.	7.6	54
21	First prototyping of a dedicated PET system with the hemisphere detector arrangement. Physics in Medicine and Biology, 2019, 64, 065004.	3.0	31
22	In vivo binding of a tau imaging probe, [11C]PBB3, in patients with progressive supranuclear palsy. Movement Disorders, 2019, 34, 744-754.	3.9	36
23	Tau imaging detects distinctive distribution of tau pathology in ALS/PDC on the Kii Peninsula. Neurology, 2019, 92, e136-e147.	1.1	19
24	[11C](R)-Rolipram positron emission tomography detects DISC1 inhibition of phosphodiesterase type 4 in live Disc1 locus-impaired mice. Journal of Cerebral Blood Flow and Metabolism, 2019, 39, 1306-1313.	4.3	3
25	Histamine H3 receptor density is negatively correlated with neural activity related to working memory in humans. EJNMMI Research, 2018, 8, 48.	2.5	6
26	Neuromolecular basis of faded perception associated with unreality experience. Scientific Reports, 2018, 8, 8062.	3.3	2
27	Tau-induced focal neurotoxicity and network disruption related to apathy in Alzheimer's disease. Journal of Neurology, Neurosurgery and Psychiatry, 2018, 89, 1208-1214.	1.9	30
28	Association between Aβ and tau accumulations and their influence on clinical features in aging and Alzheimer's disease spectrum brains: A [¹¹ C]PBB3â€PET study. Alzheimer's and Dementia: Diagnosis, Assessment and Disease Monitoring, 2017, 6, 11-20.	2.4	66
29	729. Delayed-Onset Psychosis following TBI is Associated with Tau Depositions in the Neocortex but Not with 12-Amyloid Depositions: A Pet Study with [11C]PBB3 and [11C]PiB. Biological Psychiatry, 2017, 81, S295-S296.	1.3	1
30	PET Quantification of the Norepinephrine Transporter in Human Brain with (<i>S,S</i>)- ¹⁸ F-FMeNER-D ₂ . Journal of Nuclear Medicine, 2017, 58, 1140-1145.	5.0	18
31	950. Increased Pet-Detectable Tau Pathologies in Late-Life Depression with Psychosis. Biological Psychiatry, 2017, 81, S384-S385.	1.3	0
32	Affinity States of Striatal Dopamine D2 Receptors in Antipsychotic-Free Patients with Schizophrenia. International Journal of Neuropsychopharmacology, 2017, 20, 928-935.	2.1	20
33	[ICâ€Pâ€198]: FIRSTâ€INâ€HUMAN PET STUDY WITH ¹⁸ Fâ€AMâ€PBB3 AND ¹⁸ Fâ€PN Alzheimer's and Dementia, 2017, 13, P146.	/lâ€₽₿₿3. 0.8	10
34	Visual evaluation of kinetic characteristics of PET probe for neuroreceptors using a two-phase graphic plot analysis. Annals of Nuclear Medicine, 2017, 31, 273-282.	2.2	2
35	Normative data of dopaminergic neurotransmission functions in substantia nigra measured with MRI and PET: Neuromelanin, dopamine synthesis, dopamine transporters, and dopamine D2 receptors. NeuroImage, 2017, 158, 12-17.	4.2	19
36	Measurement of psychological state changes at low dopamine transporter occupancy following a clinical dose of mazindol. Psychopharmacology, 2017, 234, 323-328.	3.1	7

#	Article	IF	CITATIONS
37	Norepinephrine Transporter in Major Depressive Disorder: A PET Study. American Journal of Psychiatry, 2017, 174, 36-41.	7.2	38
38	Comparison of two PET radioligands, [11C]FPEB and [11C]SP203, for quantification of metabotropic glutamate receptor 5 in human brain. Journal of Cerebral Blood Flow and Metabolism, 2017, 37, 2458-2470.	4.3	21
39	[P3–378]: FIRSTâ€INâ€HUMAN PET STUDY WITH ¹⁸ Fâ€AMâ€PBB3 AND ¹⁸ Fâ€PMâ€ Alzheimer's and Dementia, 2017, 13, P1104.	PBB3.	4
40	Occupancy of Norepinephrine Transporter by Duloxetine in Human Brains Measured by Positron Emission Tomography with (S,S)-[18F]FMeNER-D2. International Journal of Neuropsychopharmacology, 2017, 20, 957-962.	2.1	35
41	A human PET study of [11C]HMS011, a potential radioligand for AMPA receptors. EJNMMI Research, 2017, 7, 63.	2.5	17
42	Anatomical relationships between serotonin 5-HT2A and dopamine D2 receptors in living human brain. PLoS ONE, 2017, 12, e0189318.	2.5	8
43	PET imaging-guided chemogenetic silencing reveals a critical role of primate rostromedial caudate in reward evaluation. Nature Communications, 2016, 7, 13605.	12.8	96
44	Development of TASP0410457 (TASP457), a novel dihydroquinolinone derivative as a PET radioligand for central histamine H3 receptors. EJNMMI Research, 2016, 6, 11.	2.5	15
45	A new method to quantify tau pathologies with 11C-PBB3 PET using reference tissue voxels extracted from brain cortical gray matter. EJNMMI Research, 2016, 6, 24.	2.5	19
46	[11C]TASP457, a novel PET ligand for histamine H3 receptors in human brain. European Journal of Nuclear Medicine and Molecular Imaging, 2016, 43, 1653-1663.	6.4	13
47	PET Quantification in Molecular Brain Imaging Taking into Account the Contribution of the Radiometabolite Entering the Brain. , 2016, , 219-228.		0
48	Development of the helmet-chin PET prototype. , 2015, , .		14
49	PET Quantification of Tau Pathology in Human Brain with ¹¹ C-PBB3. Journal of Nuclear Medicine, 2015, 56, 1359-1365.	5.0	92
50	Evaluation of semi-quantitative method for quantification of dopamine transporter in human PET study with 18F-FE-PE2I. Annals of Nuclear Medicine, 2015, 29, 697-708.	2.2	9
51	Identification of a major radiometabolite of [11 C]PBB3. Nuclear Medicine and Biology, 2015, 42, 905-910.	0.6	37
52	Norepinephrine transporter occupancy by nortriptyline in patients with depression: a positron emission tomography study with (S,S)-[18F]FMeNER-D2. International Journal of Neuropsychopharmacology, 2014, 17, 553-560.	2.1	22
53	Reproducibility of PET measurement for presynaptic dopaminergic functions using L-[β-11C]DOPA and [18F]FE-PE2I in humans. Nuclear Medicine Communications, 2014, 35, 231-237.	1.1	14
54	Quantitative Analysis of Amyloid Deposition in Alzheimer Disease Using PET and the Radiotracer 11C-AZD2184. Journal of Nuclear Medicine, 2014, 55, 932-938.	5.0	17

#	Article	IF	CITATIONS
55	Biodistribution and radiation dosimetry in humans of [11C]FLB 457, a positron emission tomography ligand for the extrastriatal dopamine D2 receptor. Nuclear Medicine and Biology, 2014, 41, 102-105.	0.6	5
56	Test-retest reproducibility of dopamine D2/3 receptor binding in human brain measured by PET with [11C]MNPA and [11C]raclopride. European Journal of Nuclear Medicine and Molecular Imaging, 2013, 40, 574-579.	6.4	22
57	A MRI-based PET attenuation correction with μ-values measured by a fixed-position radiation source. , 2013, , .		О
58	Superiority illusion arises from resting-state brain networks modulated by dopamine. Proceedings of the United States of America, 2013, 110, 4363-4367.	7.1	30
59	Occupancy of serotonin and norepinephrine transporter by milnacipran in patients with major depressive disorder: a positron emission tomography study with [11C]DASB and (S,S)-[18F]FMeNER-D2. International Journal of Neuropsychopharmacology, 2013, 16, 937-943.	2.1	36
60	Quantification of Dopamine Transporter in Human Brain Using PET with ¹⁸ F-FE-PE2I. Journal of Nuclear Medicine, 2012, 53, 1065-1073.	5.0	76
61	Quantification of metabotropic glutamate subtype 5 receptors in the brain by an equilibrium method using 18F-SP203. Neurolmage, 2012, 59, 2124-2130.	4.2	13
62	Association between Striatal Subregions and Extrastriatal Regions in Dopamine D1 Receptor Expression: A Positron Emission Tomography Study. PLoS ONE, 2012, 7, e49775.	2.5	2
63	Striatal and extrastriatal dopamine D2 receptor occupancy by the partial agonist antipsychotic drug aripiprazole in the human brain: a positron emission tomography study with [11C]raclopride and [11C]FLB457. Psychopharmacology, 2012, 222, 165-172.	3.1	20
64	Synthesis and Evaluation of Radioligands for Imaging Brain Nociceptin/Orphanin FQ Peptide (NOP) Receptors with Positron Emission Tomography. Journal of Medicinal Chemistry, 2011, 54, 2687-2700.	6.4	62
65	Brain and Whole-Body Imaging in Rhesus Monkeys of ¹¹ C-NOP-1A, a Promising PET Radioligand for Nociceptin/Orphanin FQ Peptide Receptors. Journal of Nuclear Medicine, 2011, 52, 1638-1645.	5.0	50
66	Biodistribution and radiation dosimetry of a positron emission tomographic ligand, 18F-SP203, to image metabotropic glutamate subtype 5 receptors in humans. European Journal of Nuclear Medicine and Molecular Imaging, 2010, 37, 1943-1949.	6.4	32
67	Biodistribution and Radiation Dosimetry in Humans of a New PET Ligand, ¹⁸ F-PBR06, to Image Translocator Protein (18 kDa). Journal of Nuclear Medicine, 2010, 51, 145-149.	5.0	42
68	Blood Pressure Lowering with Valsartan Is Associated with Maintenance of Cerebral Blood Flow and Cerebral Perfusion Reserve in Hypertensive Patients with Cerebral Small Vessel Disease. Journal of Stroke and Cerebrovascular Diseases, 2010, 19, 85-91.	1.6	18
69	Functional brain areas associated with manipulation of a prehensile tool: A PET study. Human Brain Mapping, 2009, 30, 2879-2889.	3.6	13
70	Statistical Parametric Analysis of Cerebral Blood Flow in Vascular Dementia with Small-Vessel Disease Using ^{99m} Tc-HMPAO SPECT. Cerebrovascular Diseases, 2008, 26, 556-562.	1.7	18
71	Cerebral Hemodynamics and Oxygen Metabolism in Patients with Moyamoya Syndrome Associated with Atherosclerotic Steno-Occlusive Arterial Lesions. Cerebrovascular Diseases, 2008, 26, 9-15.	1.7	19
72	Metabotropic Glutamate Subtype 5 Receptors Are Quantified in the Human Brain with a Novel Radioligand for PET. Journal of Nuclear Medicine, 2008, 49, 2042-2048.	5.0	57

#	Article	IF	CITATIONS
73	Chronic Middle Cerebral Artery Occlusion: A Hemodynamic and Metabolic Study with Positron-Emission Tomography. American Journal of Neuroradiology, 2008, 29, 1841-1846.	2.4	36
74	Hemodynamic Influences of Azelnidipine, a Novel Calcium Channel Blocker, on Cerebral Circulation in Hypertensive Patients with Ischemic White Matter Lesions. Hypertension Research, 2008, 31, 2147-2154.	2.7	11
75	Functional brain areas involved in the use of chopsticks: A PET study. Neuroscience Research, 2007, 58, S212.	1.9	0
76	Crossed cerebellar diaschisis: a positron emission tomography study withl-[methyl-11C]methionine and 2-deoxy-2-[18F]fluoro-d-glucose. Annals of Nuclear Medicine, 2007, 21, 109-113.	2.2	33
77	N-isopropyl-4-[1231]iodoamphetamine (1231-IMP) products: a difference in radiochemical purity, unmetabolized fraction, and octanol extraction fraction in arterial blood and regional brain uptake in rats. Annals of Nuclear Medicine, 2007, 21, 387-391.	2.2	7
78	Effect of linearization correction on statistical parametric mapping (SPM): A99mTc-HMPAO brain perfusion SPECT study in mild Alzheimer's disease. Annals of Nuclear Medicine, 2006, 20, 511-517.	2.2	11
79	Diastolic blood pressure influences cerebrovascular reactivity measured by means of123I-iodoamphetamine brain single photon emission computed tomography in medically treated patients with occlusive carotid or middle cerebral artery disease. Annals of Nuclear Medicine, 2006, 20. 209-215.	2.2	4
80	Hzf protein regulates dendritic localization and BDNF-induced translation of type 1 inositol 1,4,5-trisphosphate receptor mRNA. Proceedings of the National Academy of Sciences of the United States of America, 2005, 102, 17190-17195.	7.1	24
81	Hemodynamic Influences of Losartan on the Brain in Hypertensive Patients. Hypertension Research, 2005, 28, 43-49.	2.7	30
82	Cerebrovascular collaterals and misery perfusion in patients with middle cerebral artery occlusion: A combined study with PET and angiography. Journal of Cerebral Blood Flow and Metabolism, 2005, 25, S342-S342.	4.3	0
83	Spectral analysis of99mTc-HMPAO for estimating cerebral blood flow: A comparison with H2 15O PET. Annals of Nuclear Medicine, 2004, 18, 243-249.	2.2	5
84	Cerebral hemodynamics and metabolism in adult moyamoya disease: Comparison of angiographic collateral circulation. Annals of Nuclear Medicine, 2004, 18, 115-121.	2.2	63
85	Cerebral and Cerebellar Activation in Power and Precision Grip Movements: An H215O Positron Emission Tomography Study. Journal of Cerebral Blood Flow and Metabolism, 2003, 23, 1378-1382.	4.3	15
86	Ipsilateral Hemiplegia in a Lateral Medullary Infarct— Opalski's Syndrome. , 2003, 13, 83-84.		3
87	Pharmacokinetics of active vitamins D3, 1 alpha-hydroxyvitamin D3 and 1 alpha, 25-dihydroxyvitamin D3 in patients on chronic hemodialysis. Clinical Nephrology, 1991, 35, 72-7.	0.7	17
88	Age-related increase of monoamine oxidase B in amyloid-negative cognitively unimpaired elderly subjects. Annals of Nuclear Medicine, 0, , .	2.2	0
89	Measurement of Striatal Dopamine Release Induced by Neuropsychological Stimulation in Positron Emission Tomography With Dual Injections of [11C]Raclopride. Frontiers in Psychiatry, 0, 13, .	2.6	0